Applied Catalysis B: Environmental 134–135 (2013) 302–309

Contents lists available at SciVerse ScienceDirect

Applied Catalysis B: Environmental

journal homepage: www.elsevier.com/locate/apcatb

From biomass to pure hydrogen: Electrochemical reforming of bio-ethanol in a PEM electrolyser

A. Caravaca, A. de Lucas-Consuegra*, A.B. Calcerrada, J. Lobato, J.L. Valverde, F. Dorado

Departamento de Ingeniería Química, Facultad de Ciencias y Tecnologías Químicas, Universidad de Castilla-La Mancha, Avenida Camilo José Cela 12, 13005 Ciudad Real, Spain

ARTICLE INFO

Article history:
Received 10 December 2012
Received in revised form 3 January 2013
Accepted 7 January 2013
Available online 26 January 2013

Keywords:
H_2 production
Electro-reforming
Electrolysis
Bioethanol
PEM electrolysis
Electrocatalysis

ABSTRACT

This study reports, for the first time in literature, the electrochemical reforming of a 2nd generation bio-ethanol solution (a real waste of the wine industry) for pure hydrogen production in a low temperature PEM electrolysis cell. Thereby, the main reaction parameters were studied and optimized in order to enhance the hydrogen production rate at the cathodic side of the cell. Moreover, long-term reaction experiments were carried out, together with some regeneration steps, in order to study the behavior of this system for its possible practical application. The observed reversible deactivation was discussed and supported by the electrochemical and the physico-chemical characterization of the electrodes. The results demonstrated that the origin of the observed deactivation was due to an increase in the polarization resistance of the anode due to the adsorption of reaction intermediates that can be removed by electro-oxidation during the regeneration step of the anode. The durability of the electrodes under the bioethanol electro-reforming conditions was also demonstrated in terms of thermal degradation and catalyst morphology modification. These results demonstrate the potential interest of a novel route for pure hydrogen production from biomass via electrochemical reforming.

1. Introduction

Nowadays, hydrogen could be considered as the most promising energy carrier for providing a clean, reliable and sustainable energy system. It could offer an answer to the threat of global climate change and avoid undesirable issues associated with the use of fossil fuels [1]. Then, among the different sources for hydrogen production, ethanol presents important advantages, such as natural availability, storage and handling safety. Thereby, ethanol is harmless to humans and can be easily transported and stored [2]. It can be produced renewably from several biomass sources, including energy plants, waste materials from agro industries or forestry residue materials, organic fraction of municipal solid waste, etc. [3]. Concerning the process for hydrogen production from ethanol and bioethanol, chemical catalytic reactions, such as the catalytic steam reforming (SR), have received significant attention in the literature as a promising way to produce hydrogen from renewable resources, as recently revised in previous papers [4–6]. This process led to the production of a mixture of H_2 and carbon derived products (CO and CO_2) under high reaction temperature conditions (above 500 °C). Then, further separation and purification processes are required in order to obtain high quality hydrogen for electrical energy production in fuel cells. In addition, in most of these previous studies of SR, a synthetic ethanol/water mixture has been used. Nevertheless, the qualification of "clean" fuel is only true when the raw material is biomass, which consumes CO_2 during its growth (e.g. bio-ethanol). Among the different classification of bio-ethanol, it can be differenced between 1st and 2nd generation bio-ethanol. The difference is the source of feedstock. 1st generation feedstocks are for instance corn, sugarcane and crops, whereas 2nd generation feedstocks could be agricultural waste, wood or household waste [7]. Contrary to 1st generation bio-ethanol, 2nd generation one significantly reduces greenhouse gas emissions from fuels [8] and hence there is a significant growing interest in the valorization of this kind of streams.

On the other hand, during the last years the electrolysis process has gained much attention vs. chemical catalytic processes for hydrogen production, since it allows producing pure hydrogen quick and conveniently. In addition, these processes are compatible with renewable technologies (and hence it can be used to adjust/store electrical energy consumption and demand via H_2 production). Hence, recent studies have shown promising results regarding the electrolysis (also called electro-reforming or electrochemical reforming) of alcohols: methanol [9–12] and glycerol [13,14]. Moreover, a recent study carried out by our group has also shown very promising results in the electro-reforming of ethanol/water solutions [15]. All of these studies

* Corresponding author. Tel.: +34 926 295300; fax: +34 926 295437.
E-mail address: Antonio.Lconsuegra@uclm.es (A. de Lucas-Consuegra).

0926-3373/$ – see front matter © 2013 Elsevier B.V. All rights reserved.
http://dx.doi.org/10.1016/j.apcatb.2013.01.033

Table 1
Gas chromatographic analysis of the raw bioethanol material.

	Molecular formula	Concentration (ppm)
Acetaldehyde	C_2H_4O	1983.6
Ethyl Acetate	$C_4H_8O_2$	10,087.1
1,1-Diethoxyethane	$C_6H_{14}O_2$	1550.5
Ethyl butirate	$C_6H_{12}O_2$	9.5
Methanol	CH_4O	9636.2
Allyl alcohol	C_3H_6O	123.7
1-Propanol	C_3H_8O	7513.1
1-Butanol	$C_4H_{10}O$	361.9
2-Butanol	$C_4H_{10}O$	1320.2
Iso-butanol	$C_4H_{10}O$	1550.0
3-Methyl-1-butanol	$C_5H_{12}O$	9790.6
Water	H_2O	231,100.0
Ethanol	C_2H_6O	724,973.6

have been performed in low temperature Proton Exchange Membrane (PEM) configurations, consisting of a Nafion or Sterion proton exchange membrane, leading therefore for the simultaneous production/separation of hydrogen. These studies have shown very interesting properties for the upgrading of alcohols toward the hydrogen production by electrical energy. In addition, they present several advantages respect to the water electrolysis process such as lower power electricity demands, since part of the energy required for the electrolysis is provided by the organic molecule (alcohol)

In this work, we have investigated for the first time, the electrochemical reforming of a real 2nd generation bio-ethanol from the wine industry as a novel process for producing pure H_2 from biomass. Thus, we have studied the influence of the reaction temperature and composition on the performance of the system. In addition, long-term reaction experiments were carried out together with in situ and ex situ characterization techniques in order to investigate the deactivation of the system in view of its possible practical application.

2. Experimental

2.1. Bio-ethanol source and composition

The bio-ethanol used in the present study was obtained as a residue of the distillation processes of the wine industry provided by Alcoholera Vinícola S.A., ALVINESA (Ciudad Real, Spain). Then, since it proceeds from an agricultural waste, it could be considered as a 2nd generation bio-ethanol.

A Karl Fischer titrator (701 KF Titrino) was used to determine the water concentration in the raw bio-ethanol. It was found to be 23.1% w/w. On the other hand, a complete analysis of the supplied bio-ethanol stream was carried out by using gas chromatography (BRUKER 450-GC). The results are shown in Table 1. It can be observed that, beside the main component (ethanol), the bio-ethanol stream had an important amount of water along with other higher alcohols (C_{3+}), ethyl acetate and acetaldehyde. These kinds of impurities depend on the bio-ethanol feedstock and could strongly affect the activity of the catalyst. Hence, the use of this kind of real streams is of great importance in order to critically evaluate the performance of these Electrochemical Reforming systems.

2.2. Design and operation of the PEM electrolysis system

The preparation of the membrane electrode assembly (MEA) and the design of the electrolysis unit were described in detail elsewhere [15]. Briefly, a bimetallic alloy of Pt/Ru (40% Pt–20% Ru/C-Alfa Aesar) and Pt supported on carbon (20% Pt/C-Alfa Aesar) were used as the anode and cathode electro-catalysts, respectively. These catalysts showed a good performance in our previous study for the electro-reforming of ethanol-water solutions. The inks prepared with the catalyst powder and the Nafion solution were applied on Carbon Paper substrates to achieve a metal loading of 3 mg/cm^2 for the anode, and 0.5 mg/cm^2 for the cathode. The geometric surface area of both electrodes was 6.25 cm^2. A proton conducting Sterion membrane of 185 mm thickness (Hydrogen Works) was used as the electrolyte. Prior to use, the membrane was pretreated by successive immersion at 100 °C for 2 h in H_2O_2 and H_2SO_4 solutions and deionized water. The MEA was prepared with hot-pressing, under 1 metric ton at 120 °C for 3 min.

The PEM electrolysis cell and the experimental setup were also described in our previous study [15]. PEM systems based on perfluorosulphonated materials as electrolyte need to be hydrated in order to be proton conductors, limiting the operational temperature to 90 °C at atmospheric pressure [16,17]. Hence, all the cell experiments were performed at temperatures below 80 °C. The anode compartment of the cell was supplied with ethanol and bio-ethanol water solutions of different concentrations, while water was supplied to the cathode to maintain the humidity of the membrane, as above mentioned. Anode feed flow rate was kept at 330 ml/h, while the cathode feed flow rate was kept at 10 ml/h. These flow rates were identical to the ones used in our previous study [15]. In this latter, it was demonstrated that the anodic flow rate was enough to avoid mass transfer limitations in the ethanol electrolysis, while the cathodic flow rate was enough to keep the humidity of the membrane. Constant potentials were applied to the cell via a DC power supply (DELTA ELEKTRONIKA POWER SUPPLY ES 015-10), which was also used for monitoring the current flowing through the cell. Moreover, long-term reaction experiments were carried out with a potentiostat–galvanostat Autolab PGSTAT30 (Ecochemie, The Netherlands). The outlets of both anode and cathode compartments were passed through cooling condensation columns (6 °C) in order to separate liquid and gas phase species. The flow rate of hydrogen production was also followed by gas-volume measurements and crosschecked via Faraday's Law calculations based on the cell current.

2.3. Characterization measurements

Impedance spectra were recorded by the Frequency Response Analyzer (FRA) Module of the potentiostat/galvanostat PGSTAT30 at a potential of 0.8 V. Frequency ranged from 10 kHz down to 10 mHz, with a potential wave of 0.08 V.

Termogravimetric analysis (TGA) of the cell electrodes was carried out in a TGA apparatus (TGA-DSC 1, METTLER TOLEDO). The experimental errors in the weight loss and temperature measurements were ±0.5% and ±2 °C, respectively. The TGA of the anodic catalyst was carried out under a typical electrochemical reforming reaction atmosphere of a 4 M bio-ethanol solution. It was performed by saturating a 100 mL min^{-1} N_2 stream in this solution at room temperature. The sample to be analyzed underwent a heating ramp of 2 °C min^{-1} from 50 to 100 °C, then it was kept at the latter temperature for 1 h. The TGA of the cathodic catalyst was also carried out under the same reaction atmosphere to study the thermal degradation of this electrode due to the possible crossover of the bio-ethanol solution during PEM electrochemical reforming experiments.

X-ray diffraction analysis of the fresh and of the used electrodes after electrochemical reforming experiments were recorded on a Siemens Bruker D5000 XRD Diffractometer, using Cu $K_{\alpha\alpha}$ radiation (λ = 1.54184 Å).

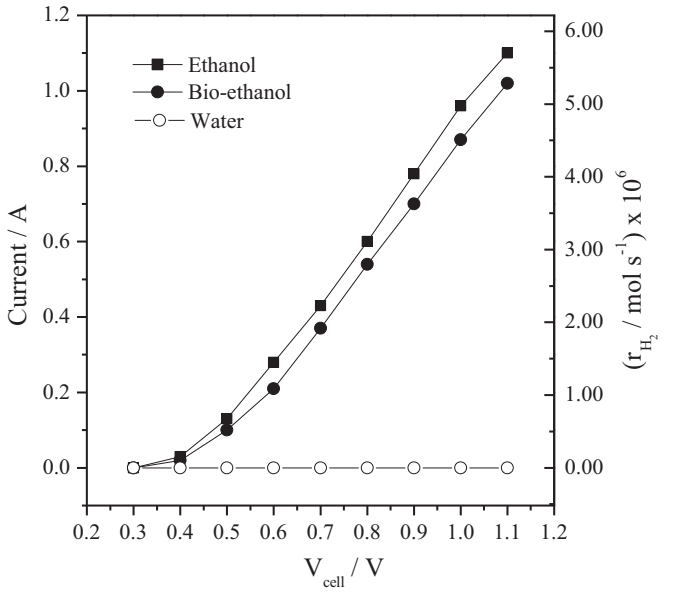

Fig. 1. Influence of the applied potential on the obtained current and the theoretical H_2 production rate for a 6 M ethanol/water, 6 M bio-ethanol/water solutions, and for distillated water. Temperature = 80 °C.

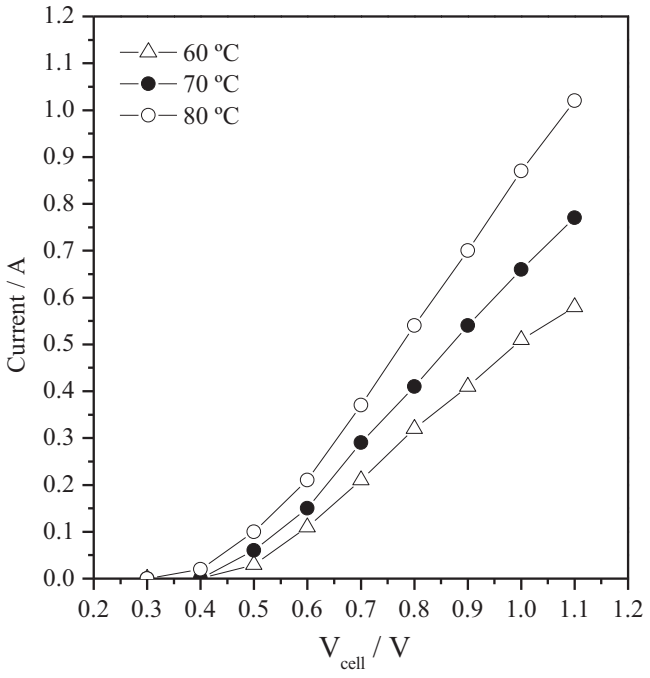

Fig. 2. Influence of the applied potential and the working temperature on the obtained current. Conditions: bio-ethanol concentration = 6 M, temperature = 60–80 °C.

3. Results and discussion

3.1. Influence of the operation parameters

In order to demonstrate the viability of the electrochemical reforming of bio-ethanol/water solutions, a typical potentiostatic experiment was carried out. It was performed under the application of step changes in the applied potential from 0 to 1.1 V at a constant temperature of 80 °C. Fig. 1 depicts the variation of the obtained steady current with the applied potential for a 6 M concentration bio-ethanol/water solution, together with the polarization curves for a 6 M ethanol/water solution and pure deionized water. It can be observed that both the ethanol and the bio-ethanol solutions showed a similar trend. The obtained current could be related to the hydrogen produced in the cathodic side of the PEM configuration by the Faraday law, i.e., $rH_2 = I/nF$, where rH_2 (represented in the secondary Y axis) is the hydrogen production rate (mol s^{-1}), n is the number of transferred electrons, and F is the Faraday constant. These theoretical H_2 production rate values were experimentally confirmed by separate measurements of gas-volumetric hydrogen flows. It was demonstrated that practically 100% of the applied electrical energy was used for H_2 production. Thus, an increase in the applied potential led to higher current values and hence to an increase in the H_2 production rate for both ethanol and bio-ethanol solutions. However, no current was obtained by feeding pure deionized water to the PEM electrolysis unit, which demonstrated that the hydrogen produced in the electrochemical reforming of ethanol and bio-ethanol solutions was due to the electrochemical oxidation of the alcohol (and not to the water electrolysis). These results agree with the electro-oxidation thermodynamics of ethanol and water. Thus, while the former process was favored at potentials higher than 0.08 V, the later took place at potentials above 1.23 V [15]. Moreover, the onset potential for both alcohols was 0.4 V, which suggests that the system was kinetically limited at lower polarizations. On the other hand, it can be observed that the current was slightly lower when bio-ethanol was fed to the electrochemical system, compared with that of the synthetic ethanol solution. Taking into account the composition of the bio-ethanol (see Table 1), this finding could be attributed to the presence of the impurities. Thus, the presence of higher alcohols (C_{3+}), ethyl acetate and acetaldehyde may act as poisons for the ethanol electro-oxidation reaction [18], slightly decreasing the efficiency of the electrolysis process. These results are also in agreement with a previous work of Lobato et al. [19],who observed a slight lower performance of a high temperature PEM fuel cell when feeding bio-ethanol vs. synthetic ethanol. The obtained results have demonstrated for the first time in literature that a real bio-ethanol solution could be electrochemically reformed in a PEM configuration for H_2 production. In this sense, some previous studies have been carried out in literature related to the steam reforming of bio-ethanol solutions in order to obtain hydrogen [3,7,20,21]. However, PEM configuration presents some important advantages regarding the steam reforming process: (a) the working temperature is strongly lower (e.g., 80 °C used here vs. the steam reforming range, from 450 to 650 °C), (b) the present configuration led to the production of high purity H_2 at the cathodic side of the cell, avoiding additional separation units, and (c) it led to a compact and modular system easy to scale up by commercial PEM stacks [22].

Fig. 2 shows the polarization curves obtained for the electrochemical reforming of a 6 M bio-ethanol solution at three different reaction temperatures (60, 70 and 80 °C). Firstly, it could be observed that no mass transfer limitations occurred at any temperature, since it was not observed a limiting current at the potential range studied [23]. As expected, an increase in the reaction temperature led to an increase of the current, enhancing therefore the hydrogen production rate in the cathode of the electrochemical cell. This phenomenon could be attributed to both, the increase of the ionic conductivity of the membrane and, on the other hand, the enhancement of the kinetics of the electrochemical reforming reactions with the working temperature [15,23].

Fig. 3 depicts the variation of the current-potential curves with the feeding bio-ethanol solution concentration at a fixed temperature of 80 °C. Mass transfer limitations could be observed at high potentials for the 2 M bio-ethanol concentration, since the system appeared to attain a limiting current. In this sense, as explained in our previous study [15], at high potentials and high current densities the system started to be limited by ohmic losses and by surface

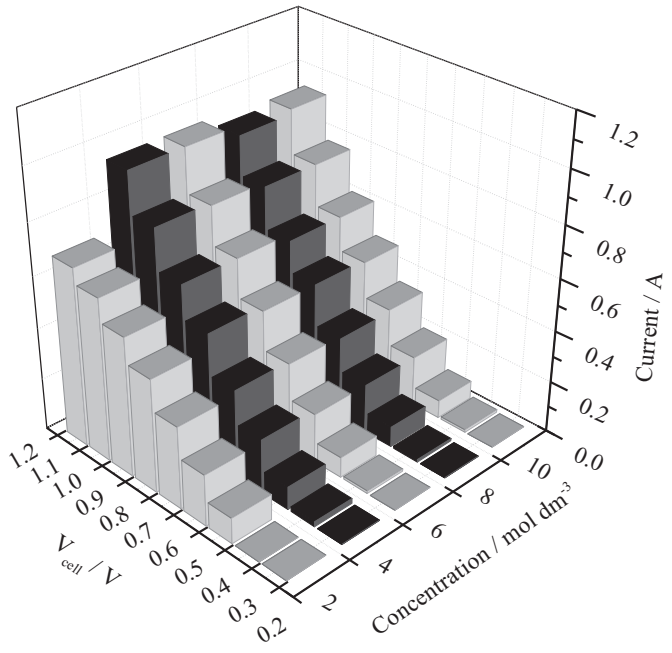

Fig. 3. Influence of the applied potential and the ethanol concentration on the obtained current. Conditions: bio-ethanol concentration = 2–10 M, temperature = 80 °C.

phenomenon (mass transfer), and hence an important effect of ethanol concentration was observed. It could explain the mass transfer limitations observed at the lowest studied bio-ethanol concentration. However, as expected, this mass transfer limitation disappeared at higher bio-ethanol concentrations (4–6 M). A further increase in the bio-ethanol concentration (>6 M) did not increase the current at fixed potential; it even slightly decreased at high concentrations (10 M). This effect can be attributed to a decrease in the membrane ionic conductivity at high alcohols concentrations, as already reported for the case of methanol [9] and ethanol [15]. According to these experiments, it was selected an optimum temperature of 80 °C and a bio-ethanol concentration of 4 M for the next deactivation and regeneration study experiments.

3.2. Deactivation and regeneration study

In order to demonstrate the viability for the practical application of the studied system, long-time electrochemical reforming experiments were carried out. These experiments were performed under the application of a constant potential of 0.8 V during 6 h at the previously studied optimal conditions (80 °C and 4 M bio-ethanol concentration). Fig. 4(a) and (b) depicts the variation of the current obtained at this potential with the time on stream. Between both long-term electrochemical reforming experiments, some regeneration cycles were carried out, which will be deeply explained below. Both Fig. 4(a) and (b) shows a pronounced decrease of the current with the time on stream during the first 4 h of the experiment. After this time, the response of the system seems to approach to a more or less steady state value. Thus, the electrochemical cell was strongly deactivated during the first 4 h of the experiment (Fig. 4a). However, after the regeneration steps, the system was almost completely reactivated leading to a second similar trend (Fig. 4b) in agreement with previous results obtained with synthetic ethanol/water solutions [15]. The observed deactivation process with the time on stream could be explained on the basis of the following processes: Firstly, the crossover of the bio-ethanol. In this sense, the crossover of ethanol from the anode to the cathode in DEFCs has been quantified in a number of publications [24,25]. As reported by Andreadis and Tsiakaras [26], in the range of ethanol concentration between 0.0 and 8.0 mol L^{-1}, the crossover rate is linearly increased along with the ethanol feed concentration increment. Then, one of the major problems associated with crossover is the creation of a mixed potential at the cathode due to simultaneous reduction of oxygen and oxidation of ethanol [27]. However, under the electrolysis mode, no O_2 was introduced at the cathodic side of the PEM electrolysis cell, avoiding this oxidation reaction and decreasing therefore this main influence of the crossover on the performance of the cell. Moreover, the membrane swelling [25,28–30], and the poisoning of the anodic electrochemical catalysts due to the adsorption of some reaction intermediates [19,31] produced during the electro-reforming process could led to the observed deactivation phenomena. However, the deactivation of the cell was completely reversible after the regeneration step. Hence, the catalyst poisoning by the adsorption of reaction intermediates seemed to be the most plausible reason. Moreover, an empiric model was used to study the deactivation of this system. This model was described elsewhere [15]. Briefly, it defines the evolution of the current with the time on stream under the application of a constant cell potential as follows:

$$\frac{I_t - I_0}{I_{ss} - I_0} = \frac{\Delta t}{\beta + \Delta t} \quad (1)$$

where I_t, I_0 and I_{ss} are the cell current at time t and $t = 0$, and under steady-state conditions, respectively; Δt is the time increment, and β is the deactivation constant. Then, inset of Fig. 4(a) and (b) shows the variation of the "y" factor defined as $(y = (I_{ss} - I_0)/(I_t - I_0))$ vs. Δt^{-1} for both experiments carried out under constant polarization conditions. As it can be observed, this model properly predicted the behavior of this system. Thus, the deactivation constant for both experiments was $\beta = 0.83$. This value is similar to that reported in our previous study with ethanol under similar reaction conditions ($\beta = 0.85$), which again demonstrates that this system depicted a similar behavior respect to the ethanol/water solutions. Hence, it seems that the high concentration of impurities presented in the bio-ethanol stream did not strongly affect the observed deactivation behavior in comparison with a synthetic ethanol/water stream. The obtained steady state current was around 0.21 A (33.6 mA cm^{-2}) at 0.8 V. It could be related with a hydrogen production rate of 1.09 μmol H_2 s^{-1} (1.73 mL min^{-1}), which is in agreement with the experimental gas volumetric flow measurement of 1.88 mL min^{-1}. These values correspond to an energy consumption of 21.44 kW h kg^{-1} of pure hydrogen. This value is slightly lower in comparison with the values previously reported for ethanol-water solutions in our previous study (current = 0.23 A) [15], in good agreement with the results above explained for Fig. 1.

Concerning the regeneration steps of the system between the two experiments described in Fig. 4, this regeneration procedure consisted of series of potentiostatic polarizations from 0.4 V to 1.1 V by a set of repetitive cycles carried out under exactly the same reaction conditions (80 °C and 4 M bio-ethanol concentration). Each potentiostatic transient was applied until an almost steady state current value was achieved. Fig. 5 (a) and (b) shows, for the first regeneration cycle, the variation of the current with the time on stream under different polarizations. It can be observed that starting from low potentials (Fig. 5a) and shifting to higher ones (Fig. 5b) the system showed a strong activation of the obtained current under the application of potentials higher than 0.8 V. The repetition of this regeneration cycles for several times led to a complete reactivation of the system as it can be observed in Fig. 6. This figure shows the attained steady state current at each potential for the different regeneration cycles. Regarding the first cycle, it can be observed, a strong change in the trend of the polarization

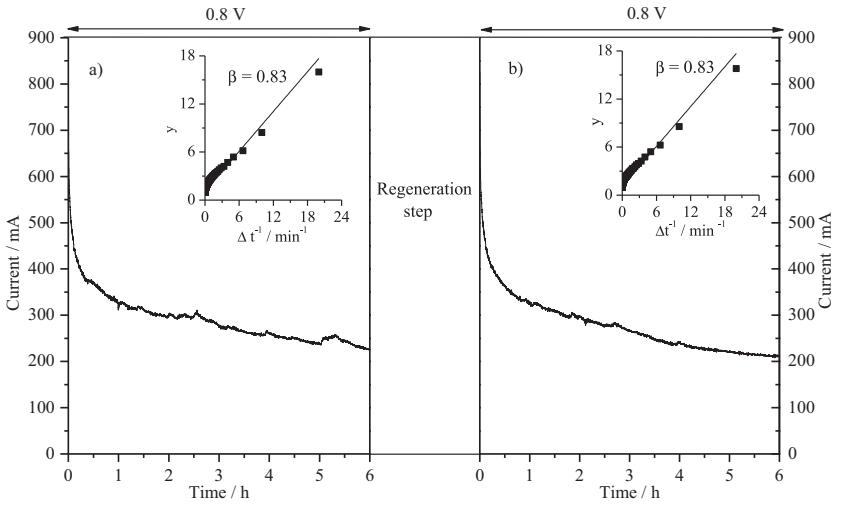

Fig. 4. Variation of the current vs. time on stream at fixed applied potential during two consecutive durability experiments and the fit to the empirical deactivation model (inset of the figure). Conditions: bio-ethanol concentration = 4 M, temperature = 80 °C. V_{cell} = 0.8 V.

curve at potentials higher than 0.8 V. Moreover, an increase of the current was obtained from the first cycle to the second one. However, after the third cycle, no important variation was observed in the subsequent polarization curves, which demonstrates that a set of three regeneration cycles is enough to completely activate the electrochemical cell for the electro-reforming of bio-ethanol solutions. This regeneration could be attributed to the electro-oxidation of the adsorbed reaction intermediates. Hence, during the long-term experiments, the cell was deactivated due to the formation of reaction intermediates (e.g., acetaldehyde), which adsorbed and blocked the anodic electro-catalyst active sites. However, as observed in the regeneration experiments, the system started to be activated under the application of high polarizations. It could be explained taking into account the role of the Ru in the anode catalyst. This metal is the responsible of the activation of the water molecules at high potentials by producing oxygen-containing species (OH) [18,32]. Then, these latter ones could lead to the removal of the adsorbed reaction intermediates, therefore activating the catalyst active sites for the electro-reforming of bio-ethanol [15].

3.3. Characterization measurements

To get more insights on the different behavior of the electrochemical cell, an analysis of the electrochemical impedance spectroscopy (EIS) was carried out for both the deactivated and the regenerated cell under the application of 0.8 V, i.e., at the end of the first long-term experiment (deactivated state) and the beginning of the second one (regenerated state). This technique can be used to measure global cell impedances, then avoiding the use of a reference electrode. Hence, the benefit of global cell impedance measurements is that they provide an in situ information about the PEM cell operating under real bio-ethanol electrolysis conditions [33].

Nyquist plots are reported for both states in Fig. 7. Following the general rules on EIS, the intercept on the real axis in the high frequency range of the spectrum corresponds to the total ohmic resistance of the cell (R_S), which can be expressed as the sum of the contributions from contact resistances between components and ohmic resistances of the cell components such as the membrane, catalyst layer, gas diffusion layer, and bipolar plates [34]. On the

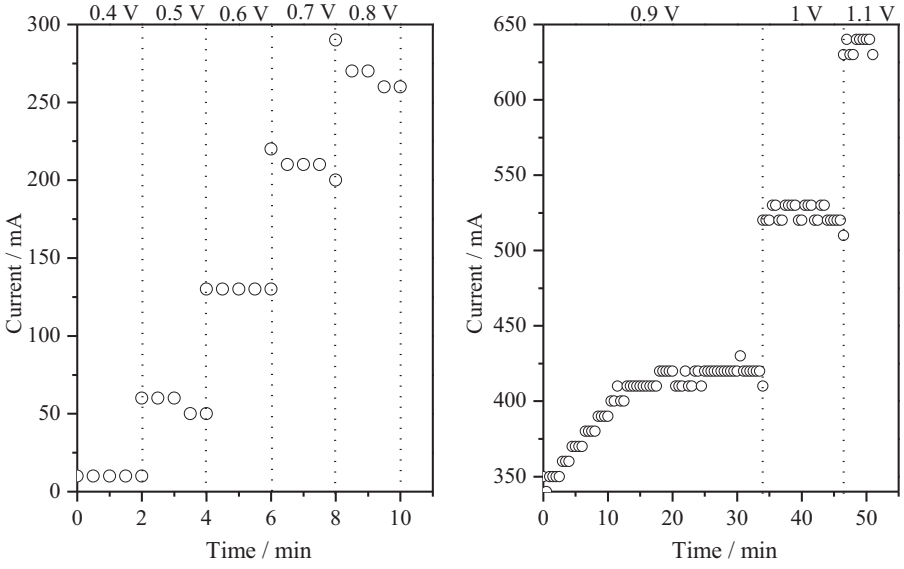

Fig. 5. Variation of the current vs. time on stream under the application of different cell potentials during the first regeneration cycle. Conditions: bio-ethanol concentration = 4 M, temperature = 80 °C. V_{cell} = 0.4–0.8 V (a) and V_{cell} = 0.9–1.1 V (b).

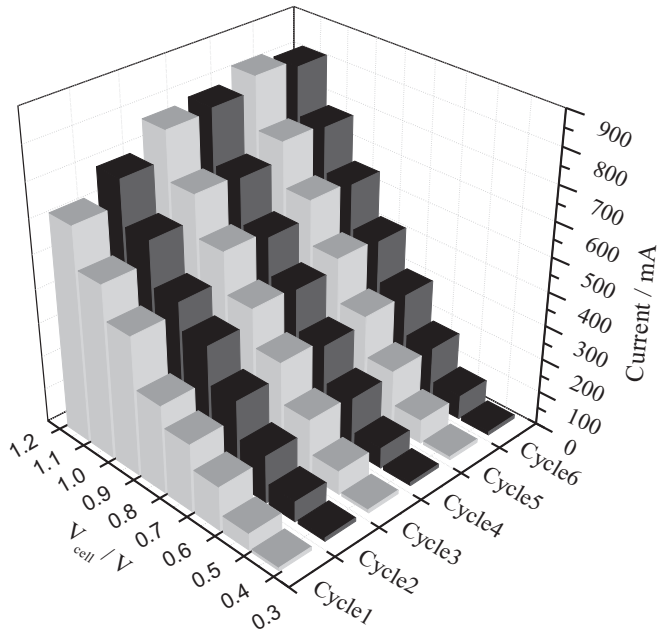

Fig. 6. Influence of the number of cycles on the current obtained under the application of different potentials. Conditions: bio-ethanol concentration = 4 M, temperature = 80 °C. V_{cell} = 0.4–1.1 V.

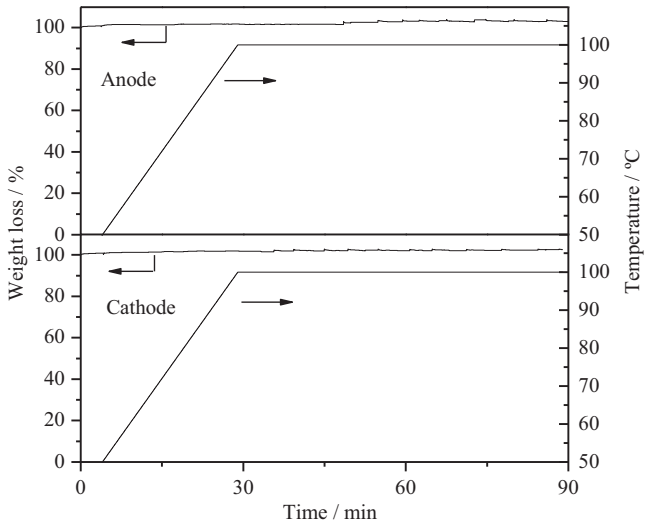

Fig. 8. Thermogravimetric analysis of the two fresh electrodes (anode and cathode) under a 4 M bio-ethanol reaction atmosphere. Conditions: N_2 flow = 100 mL min^{-1}, heating ramp: 2 °C min^{-1} from 50 to 100 °C.

other hand, the overall charge transfer resistance (anode + cathode) and the mass transport were obtained by the difference between the high frequency real *Z*-axis and the low frequency real *Z*-axis intercept (R_{CT+MT}) [35]. These resistance values for both the deactivated and regenerated cell are also summarized in the figure. The first incomplete semicircle in the high frequency region could be attributed to the distributed resistance effects in the electrolyte within the catalyst layer [36,37]. Regarding the ohmic resistance, it can be clearly observed a slight decrease of this parameter when the cell was regenerated. It could be attributed to a decrease of the ohmic resistance of the catalyst layer in the regenerated cell, but further experiments should be carried out to clarify this point. On the other hand, one can clearly observe in this figure a strong

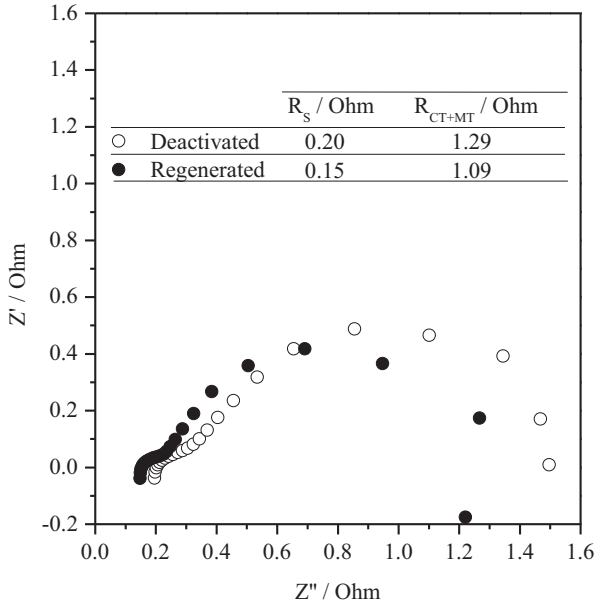

Fig. 7. Impedance spectra for the deactivated and the regenerated electrochemical cell.

decrease of the R_{CT+MT} for the regenerated cell. This resistance is defined as the sum of the kinetic and mass transfer losses of both cell electrodes. Mass transfer contribution could be avoided since no diffusional limitations were observed at the explored reaction conditions in the polarization curves performed in the previous experiments. Moreover, the hydrogen evolution at the cathodic side of the PEM electrolyzer could be considered as a fast process [35]. In this sense, in a previous study related with the water electrolysis in a PEM configuration, the electrode resistance attributed to the hydrogen evolution in the cathode was found to be three orders of magnitude lower than that for the oxygen evolution at the anode [33]. Hence, it can be assumed that the R_{CT+MT} was mainly due to the charge transfer at the anode of the cell. As expected, this resistance decreased for the regenerated electrode since the current supplied by the system at this potential increased. Thus, this technique supported the results previously obtained in the long-term and the subsequent regeneration experiments. In this sense, it seems that the deactivation of the cell was due to the block of the anode electro-catalyst active sites, leading to an increase of the polarization resistance, as observed in Fig. 7. However, during the regeneration steps, the application of potentials higher than 0.8 V led to the electro-oxidation of the intermediates adsorbed species in the catalyst active sites, in turn leading to a decrease in the polarization resistance value [38].

On the other hand, despite the anodic electro-catalyst could be mostly regenerated, one can observe slight lower current values (first experiment shown in Fig. 1) when they are compared to those depicted on the regeneration cycles of Fig. 6. It could be attributed to the swelling phenomenon, or to the degradation of the electrodes under the operation conditions. In order to study the latter phenomena, two different ex situ characterization techniques were carried out.

Firstly, thermogravimetric analysis (TGA) to a piece of both fresh electrodes (carbon paper + catalyst layer + Nafion ionomer) were performed with a 4 M bio-ethanol solution under a typical electrochemical reforming reaction atmosphere (see the conditions described in Section 2). The results are shown in Fig. 8. As can be observed, the electrodes did not undergo any important variation, demonstrating that both electrodes were stable under the reaction atmosphere (the stability of the cathode was also verified for possible crossover of bio-ethanol/solution through the membrane). However, one could think that, even though the electrodes were

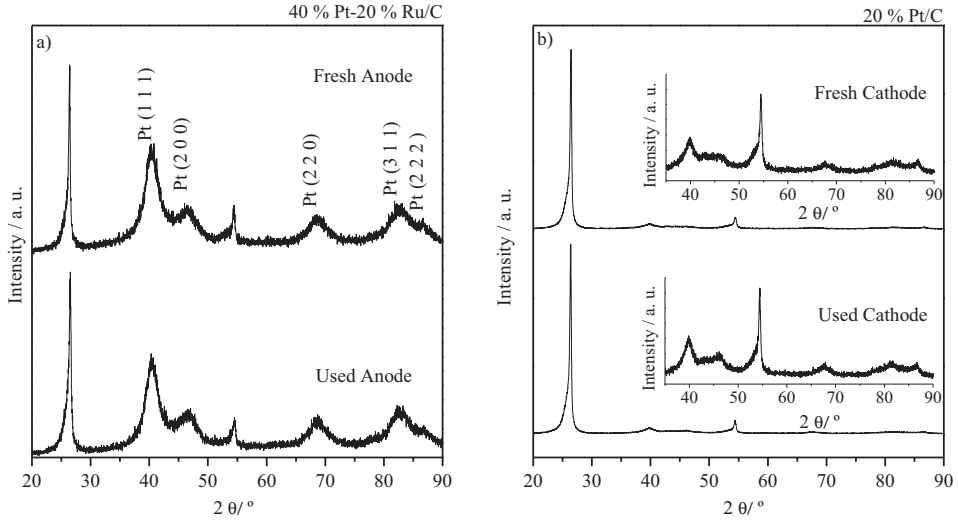

Fig. 9. X-ray diffraction patterns of the (a) fresh and used anode and (b) cathode.

Table 2
Main structural parameters obtained by the XRD analysis of the fresh electrodes.

	Pt (2 2 0) peak position, 2θ (°)	Lattice parameter (Å)	Particle size (nm)	Alloying degree (%)
Fresh Anode PtRu/C	68.55	3.868	5.1	73.7
Fresh Cathode Pt/C	67.55	3.919	10.7	–

stable under this reaction environment, they could undergo some structural changes during the long-term stability tests and the subsequent regeneration experiments explained above. Then, X-ray diffraction (XRD) experiments were performed for both fresh and used (after electro-reforming experiments) cell electrodes (Fig. 9). Two peaks at around $2\theta = 25°$ and 55° were observed in all diffractograms, which could be associated with the carbon paper used as a current collector. This fact was corroborated by the XRD spectra of this material (not shown here) and that of the catalyst support [39]. All the XRD patterns clearly showed the five main characteristic peaks of the face centered cubic (fcc) crystalline Pt, i.e., the planes (1 1 1), (2 0 0), (2 2 0), (3 1 1), and (2 2 2). No peaks related to metallic ruthenium with a hexagonal close packed (hcp) structure or the ruthenium oxide phase were observed in Fig. 9a [40]. Comparing the two electrodes (anode and cathode), one can observe a remarkable difference between the relative intensity in the XRD spectra of the carbon and Pt peaks, which could be mainly attributed to both the different catalyst loading and metallic charge of the electrocatalysts. Thereby, the diffraction peaks in the Pt-Ru/C electrocatalysts were slightly shifted to higher 2θ values with respect to the same reflections in Pt/C. These results would suggest that Ru may be incorporated into the Pt fcc structure [41], leading to the formation of a Pt-Ru/C alloy in the electrocatalysts [42,43]. The main parameters obtained from Fig. 9 for the fresh electrodes are summarized in Table 2. In order to assess both the particle size as well as verify the degree of alloy formation (for the anode catalyst), (2 2 0) reflections were analyzed. As matter of fact, it is expected that the carbon support only contributes in terms of a linear background [44].

Scherrer's law was used to determine the particle size [45]. Lattice parameters (α) were evaluated according to ref. [44] whereas the degree of alloy formation was measured taking into account the following equation [18] based on Vegard's law:

$$\alpha_{(\text{Pt-M})} = \alpha_{(\text{Pt})} - kx_{(\text{Ru})} \quad (2)$$

where $\alpha_{(\text{Pt})} = 0.3913$ nm is the lattice parameter of Pt/C catalyst, and k is a constant equal to 0.0124 nm. According to this equation, the atomic content of alloyed Ru ($x_{(\text{Ru})}$) in the anodic catalyst is 0.37, indicating that around 73.7% of this metal was alloyed with Pt.

Apart from these structural parameters analysis, one can clearly observe that the diffractograms for the fresh and used anode and cathode were exactly identical (as well as the structural parameters in each case, not shown here), leading to no morphological modifications in each electrode after the electrochemical-reforming experiments. In a previous work by Lobato et al. [46] for a high temperature PEM fuel cell, a significant increase in the catalyst particle size was observed after fuel cell testing. Contrary to that, the results presented in Fig. 9 show that the electrodes used for the electro-reforming of a bio-ethanol solution in low temperature PEM were not morphologically affected under both the operation conditions used and the long-term reaction experiments carried out.

Although the electrodes did not undergo any important thermal degradation and catalyst morphology modification during long operation times, the slight non-reversible deactivation observed could be related to swelling phenomena. However, most of the activity of this system was regenerated as described above, leading to a promising alternative for the hydrogen production by the electro-reforming of bio-ethanol solutions.

4. Conclusions

4.1. The following conclusions could be drawn from this study

- The electrochemical reforming of bio-ethanol solutions in a PEM electrolyser led to the production of pure hydrogen under the application of low polarizations (0.4–1.1 V).
- The hydrogen production was enhanced by the optimization of the main reaction parameters. Hence, the optimum conditions were found to be 80 °C, and 4 M bio-ethanol as the feed stream of this electrocatalytic system.
- Long-term experiments together with some regeneration steps were used to demonstrate that the PEM electrolyser could properly work for long operation times. Hence, although the cell

was deactivated due to the adsorption of some reaction intermediates, it was easily reactivated after three regeneration cycles.
- The electrochemical cell characterization by means of electrochemical impedance spectroscopy demonstrated the lower polarization resistance of the anode for the regenerated cell, which agreed well with the results obtained in the long-term experiments.
- The stability of the cell electrodes was characterized by TGA experiments and XRD analysis, thus demonstrating that both electrodes did not suffer any important thermal degradation and structural modification during the electrochemical reforming experiments.

Acknowledgments

We gratefully acknowledge Spanish MICINN project CTQ 2010-16179/PQ for the financial support of this work. We also thank "ALVINESA" company for supplying the raw bioethanol sample.

References

[1] R. Balaji, N. Senthil, S. Vasudevan, S. Ravichandran, S. Mohan, G. Sozhan, S. Madhu, J. Kennedy, S. Pushpavanam, M. Pushpavanam, International Journal of Hydrogen Energy 36 (2011) 1399–1403.
[2] B.S. Kwak, J. Kim, M. Kang, International Journal of Hydrogen Energy 35 (2010) 11829–11843.
[3] P. Giunta, C. Mosquera, N. Amadeo, M. Laborde, Journal of Power Sources 164 (2007) 336–343.
[4] A. Haryanto, S. Fernando, N. Murali, S. Adhikari, Energy and Fuels 19 (2005) 2098–2106.
[5] M. Ni, D.Y.C. Leung, M.K.H. Leung, International Journal of Hydrogen Energy 32 (2007) 3238–3247.
[6] P.D. Vaidya, A.E. Rodrigues, Chemical Engineering Journal 117 (2006) 39–49.
[7] J. Rass-Hansen, R. Johansson, M. Møller, C.H. Christensen, International Journal of Hydrogen Energy 33 (2008) 4547–4554.
[8] A.E. Farrell, R.J. Plevin, B.T. Turner, A.D. Jones, M. O'Hare, D.M. Kammen, Science 311 (2006) 506–508.
[9] G. Sasikumar, A. Muthumeenal, S.S. Pethaiah, N. Nachiappan, R. Balaji, International Journal of Hydrogen Energy 33 (2008) 5905–5910.
[10] C.R. Cloutier, D.P. Wilkinson, International Journal of Hydrogen Energy 35 (2010) 3967–3984.
[11] T. Take, K. Tsurutani, M. Umeda, Journal of Power Sources 164 (2007) 9–16.
[12] Z. Hu, M. Wu, Z. Wei, S. Song, P.K. Shen, Journal of Power Sources 166 (2007) 458–461.
[13] A.T. Marshall, R.G. Haverkamp, International Journal of Hydrogen Energy 33 (2008) 4649–4654.
[14] S. Kongjao, S. Damronglerd, M. Hunsom, Journal of Applied Electrochemistry 41 (2011) 215–222.
[15] A. Caravaca, F.M. Sapountzi, A. de Lucas-Consuegra, C. Molina-Mora, F. Dorado, J.L. Valverde, International Journal of Hydrogen Energy 37 (2012) 9504–9513.
[16] W.-Y. Lee, G.-G. Park, T.-H. Yang, Y.-G. Yoon, C.-S. Kim, International Journal of Hydrogen Energy 29 (2004) 961–966.
[17] J. Lobato, P. Cañizares, M.A. Rodrigo, C.-G. Piuleac, S. Curteanu, J.J. Linares, International Journal of Hydrogen Energy 35 (2010) 7889–7897.
[18] H. Li, G. Sun, L. Cao, L. Jiang, Q. Xin, Electrochimica Acta 52 (2007) 6622–6629.
[19] J. Lobato, P. Cañizares, M.A. Rodrigo, J.J. Linares, Fuel Cells 9 (2009) 597–604.
[20] A. Le Valant, F. Can, N. Bion, D. Duprez, F. Epron, International Journal of Hydrogen Energy 35 (2010) 5015–5020.
[21] A. Le Valant, A. Garron, N. Bion, D. Duprez, F. Epron, International Journal of Hydrogen Energy 36 (2011) 311–318.
[22] S. Siracusano, V. Baglio, N. Briguglio, G. Brunaccini, A. Di Blasi, A. Stassi, R. Ornelas, E. Trifoni, V. Antonucci, A.S. Aricò, International Journal of Hydrogen Energy 37 (2012) 1939–1946.
[23] J.O.M. Bockris, A.K.M. Reddy, M. Gamboa-Aldeco, Modern Electrochemistry, Kluwer Academic/Plenum, New York, 2000.
[24] G. Li, P.G. Pickup, Journal of Power Sources 161 (2006) 256–263.
[25] S. Song, G. Wang, W. Zhou, X. Zhao, G. Sun, Q. Xin, S. Kontou, P. Tsiakaras, Journal of Power Sources 140 (2005) 103–110.
[26] G. Andreadis, P. Tsiakaras, Chemical Engineering Science 61 (2006) 7497–7508.
[27] D.D. James, P.G. Pickup, Electrochimica Acta 55 (2010) 3824–3829.
[28] J.A. Elliott, S. Hanna, A.M.S. Elliott, G.E. Cooley, Polymer 42 (2001) 2251–2253.
[29] A.M. Affoune, A. Yamada, M. Umeda, Journal of Power Sources 148 (2005) 9–17.
[30] D. Rivin, C.E. Kendrick, P.W. Gibson, N.S. Schneider, Polymer 42 (2001) 623–635.
[31] S. Song, P. Tsiakaras, Applied Catalysis B 63 (2006) 187–193.
[32] H. Wang, Z. Jusys, R.J. Behm, Journal of Power Sources 154 (2006) 351–359.
[33] P. Millet, N. Mbemba, S.A. Grigoriev, V.N. Fateev, A. Aukauloo, C. Etiévant, International Journal of Hydrogen Energy 36 (2011) 4134–4142.
[34] F. Liu, B. Yi, D. Xing, J. Yu, Z. Hou, Y. Fu, Journal of Power Sources 124 (2003) 81–89.
[35] M. Mamlouk, K. Scott, Electrochimica Acta 56 (2011) 5493–5512.
[36] V.A. Paganin, C.L.F. Oliveira, E.A. Ticianelli, T.E. Springer, E.R. Gonzalez, Electrochimica Acta 43 (1998) 3761–3766.
[37] T.J.P. Freire, E.R. Gonzalez, Journal of Electroanalytical Chemistry 503 (2001) 57–68.
[38] S.Y. Cha, W.M. Lee, Journal of the Electrochemical Society 146 (1999) 4055–4060.
[39] L. Colmenares, H. Wang, Z. Jusys, L. Jiang, S. Yan, G.Q. Sun, R.J. Behm, Electrochimica Acta 52 (2006) 221–233.
[40] E.V. Spinacé, A.O. Neto, T.R.R. Vasconcelos, M. Linardi, Journal of Power Sources 137 (2004) 17–23.
[41] J.R.C. Salgado, F. Alcaide, G. Álvarez, L. Calvillo, M.J. Lázaro, E. Pastor, Journal of Power Sources 195 (2010) 4022–4029.
[42] D. Chu, S. Gilman, Journal of the Electrochemical Society 143 (1996) 1685–1690.
[43] A.S. Aricò, P. Cretì, H. Kim, R. Mantegna, N. Giordano, V. Antonucci, Journal of the Electrochemical Society 143 (1996) 3950–3959.
[44] V. Radmilovic, H.A. Gasteiger, P.N. Ross, Journal of Catalysis 154 (1995) 98–106.
[45] C. Suryanarayana, M.G. Norton, X-Ray Diffraction: a Practical Approach, Plenum, New York, NY, 1998.
[46] J. Lobato, P. Cañizares, M.A. Rodrigo, J.J. Linares, Electrochimica Acta 52 (2007) 3910–3920.